between the RhRh σ and δ^* orbitals as the SOMO. Consideration of the bond length changes that occur on oxidation, for the structures so far determined, supports the ordering of MO's outlined in this work.

Conclusion

The study of redox-related complexes that contain metal–metal bonds provides some insight into the subtleties of the bonding. This is particularly the case when the metal–metal bonding is weak and where the other perturbations to the bonding can lead to experimentally observable changes in the system. For the dirhodium complexes the metal–metal δ bonding is weak, and its effects can be nullified by changes in the σ and π interactions between the metal and the other ligands in the complex.

Contribution from the Research School of Chemistry, The Australian National University, Canberra, ACT 2601, Australia, and Department of Chemistry, Monash University, Clayton, Victoria 3618, Australia

Magnetism and Electronic Structure of a Series of Encapsulated First-Row Transition Metals

Lisandra L. Martin,*[1a] Raymond L. Martin,*[1b] Keith S. Murray,*[1b] and Alan M. Sargeson*[1a]

Received March 21, 1989

The temperature dependence of the magnetic susceptibility (4.2–300 K) is reported for a series of crystalline salts of first-row transition-metal ions encapsulated by hexaamine ligands of the sar type, namely, $[M(sar)]^{n+}$, where sar = 3,6,10,13,16,19-hexaazabicyclo[6.6.6]icosane, or $[M((X,Y)sar)]^{n+}$, where X = Y = 1,8-NH_2 1,8-NH_3^+ or X = 1-CH_3, Y = 8-H. The cage complexes of Fe^{III}, Co^{III}, and Ni^{III} all exhibit low-spin ground states [of $^2T_{2g}$ and $^1A_{1g}$ (O_h) and $^2A_{1g}$ (D_{4h}) origin] whereas that of Mn^{III} is high-spin [$^5A_{1g}$ or $^5B_{1g}$ (D_{4h})]. The complexes of Mn^{II}, Co^{II}, and Ni^{II} are high-spin [of $^6A_{1g}$, $^4T_{1g}$, and $^3A_{2g}$ (O_h) origin], but surprisingly, those of Fe^{II} exhibit either a low-spin ($^1A_{1g}$) or a high-spin ($^5T_{2g}$) ground state depending on the nature of the apical substituent and the lattice. Clearly, the magnitude of the ligand field parameters ($10Dq$ and B)† generated by these saturated macrobicycles for the $3d^6$ Fe^{II} is that required for the high-spin/low-spin crossover for six saturated amine ligands. The ground states for V^{IV} ($^2T_{2g}$), V^{III} ($^3T_{1g}$), Cr^{III} ($^4A_{2g}$), Cu^{II} ($^2B_{1g}$ in D_{4h}), and Zn^{II} ($^1A_{1g}$) appear to be unambiguous. The magnitude of the zero-field-splitting parameter has been estimated from the low-temperature $\chi(T)$ data for the Cr^{III} and high-spin Mn^{III}, Mn^{II}, Fe^{II}, Co^{II}, and Ni^{II} cage complexes. The low-spin (^2E_g origin) state for Co^{II} is stabilized by the (aza)capten ligand because of the larger nephelauxetic effect of sulfur combined with appreciable Jahn–Teller splitting of the ^2E_g ground state. The magnetic properties in general reflect the reduction in symmetry observed crystallographically for the individual metal ions.

Introduction

The synthesis[2] of an extended series of hexadentate ligands of the macrobicyclic type based on saturated nitrogen donor atoms enables the properties of their transition-metal complexes to be studied in a common environment. The macrobicyclic cage can be synthesized by capping $[Co(en)_3]^{3+}$ (en = ethane-1,2-diamine) along the C_3 axis to yield the cobalt(III) cage cation shown in Figure 1a. The free ligand can be isolated in good yield by treatment of the cobalt(II) cage with either HBr or KCN,[3] thereby enabling a range of encapsulated transition-metal ions to be synthesized.[4] Encapsulation results in transition-metal complexes that are mononuclear and kinetically inert to dissociation of the metal ion and offers the prospect of stabilizing unusual oxidation states of the metal atom.[4,5]

Single-crystal X-ray structural studies[6] of a number of the transition metal cages have established that all six secondary N atoms are bound to the metal ion and the molecular structure of the MN_6 core varies considerably with the electronic configuration and spin state of the central metal.[4] Competition between the preferred metal stereochemistry and the geometrical demands of the ligand appears to determine the overall geometry, resulting in complexes that range from near-octahedral (e.g. Co^{III}) to near-trigonal-prismatic structures (e.g. V^{IV}).[6] However, it is evident from the structural data that there are also small perturbations from the D_3 symmetry preferred by the ligand of tetragonal or rhombic origin, which may influence electronic structure and spectroscopic properties. Broadly, the metal cages fall into two groups that can be characterized crudely in terms of their trigonal twist angles, ϕ, about the C_3 axis (cf. Figure 1b): The first group (Mg^{II}, Cd^{II}, Hg^{II}, Mn^{II}, Fe^{II}, Co^{II}, Cu^{II}, Zn^{II}, Ag^{II}) has $\phi \sim 28°$ with structures similar to that of the metal-free tetraprotonated ligand $[(NH_3)_2sarH_2]^{4+}$. For the second group, the trigonal twist angle, ϕ, lies between 46 and 60° and increases in the order $Ni^{II} < Cr^{III} < Fe^{III} < Co^{III}$.[6] For the V^{IV} cage,[6,7] ϕ equals 18° and the $[Co^{II}(sep)]S_2O_6 \cdot H_2O$ structure is a special case where the ligand cap deforms in an unusual way.

A study of the temperature dependence (4–300 K) of the magnetic susceptibility of a number of transition-metal cages has been undertaken to establish the electronic configuration of their ground states and compare their magnetic behavior with that of the closely related $[M(NH_3)_6]^{n+}$, $[M(en)_3]^{n+}$, and $[M([9]aneN_3)_2]^{n+}$ complexes ([9]aneN$_3$ = 1,4,7-triazacyclononane). Although structural studies indicate that distortions from ideal octahedral geometry occur for these compounds,[6] for convenience, discussion of the magnetic data is given here in terms of ground states assumed to have their origin in octahedral MN_6 symmetry.

Experimental Section

Preparation of Complexes. All complexes were prepared either by published procedures[2-4] or methods to be published shortly and analyzed just prior to the magnetic measurements to confirm analytical purity. The complex (ca. 20–30 mg) was finely ground with an agate mortar and pestle and packed tightly into a small gold bucket. The sample and

† $10Dq$ is used here to describe the ligand-field parameters although the symmetries are lower than octahedral; Δ is used for axial distortion. Octahedral parent (or tetragonal D_{4h}) symmetry notations are generally used for convenience. This is an approximation in view of the trigonal distortion preferred by the ligand[6] and tetragonal distortions preferred by some of the metal ions.

(1) (a) The Australian National Univeristy. (b) Monash University.
(2) Geue, R. J.; Hambley, T. W.; Harrowfield, J. M.; Sargeson, A. M.; Snow, M. R. *J. Am. Chem. Soc.* **1984**, *106*, 5478.
(3) Creaser, I. I.; Gahan, L. R.; Hagen, K. S.; Harrowfield, J. M.; Lawrance, G. A.; Martin, L. L.; Sargeson, A. M.; White, A. H. Manuscript in preparation.
(4) Martin, L. L. Magnetic and Electrochemical Studies of Some Encapsulated Metal Ions. Ph.D. Thesis, The Australian National University, 1986.
(5) Sargeson, A. M. *Chem. Br.* **1979**, *15*, 23.
(6) Comba, P.; Sargeson, A. M.; Engelhardt, L. M.; Harrowfield, J. M.; White, A. H.; Horn, E.; Snow, M. R. *Inorg. Chem.* **1985**, *24*, 2325.
(7) Comba, P.; Engelhardt, L. M.; Harrowfield, J. M.; Lawrance, G. A.; Martin, L. L.; Sargeson, A. M.; White, A. H. *J. Chem. Soc., Chem. Commun.* **1985**, 174.

0020-1669/90/1329-1387$02.50/0

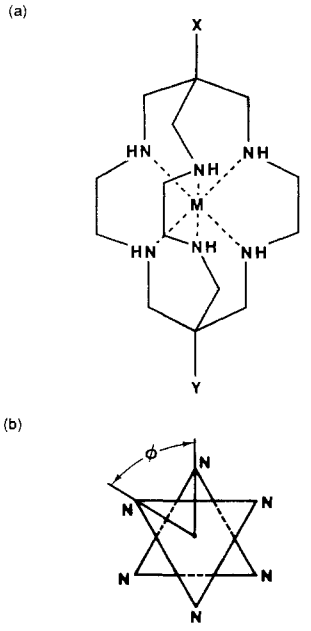

Figure 1. (a) Structure of the cage complexes $[M((X,Y)sar)]^{n+}$, where X = Y = H is $[M(sar)]^{n+}$, X = Y = NH_3 is $[M((NH_3)_2sar)]^{(n+2)}$, and X = Y = NH_2 is $[M((NH_2)_2sar)]^{n+}$. (b) Definition of twist angle ϕ. For an octahedron, $\phi = 60°$; for a trigonal prism, $\phi = 0°$.

bucket were reweighed after completion of the magnetic measurements to check for any weight loss on evacuation. Air-sensitive samples were sealed in argon-filled ampules prior to measurement. These samples were finely ground and packed into the gold bucket inside a nitrogen-filled glovebag. The samples were checked for signs of oxidation before and after the magnetic measurements.

Magnetic Susceptibility Measurements. The average mass susceptibility, χ_g, was measured with an extensively modified Oxford Instruments Faraday magnetometer with redesigned supports for the microbalance and superconducting magnets.[8] The system comprised a liquid-helium Dewar with a NbTi superconducting magnet assembly to provide the main and gradient fields, a variable-temperature insert for sample temperature control, a Sartorius microbalance (Model 4104) for force measurements, and associated vacuum facilities. The main and gradient fields were independently variable; however, usual values were 10 or 40 kG and 1000 G cm^{-1}, respectively. For Fe^{II} and Co^{II} cages, 5- and 10-kG main fields were employed in order to prevent sample alignment. Measurements were made manually between 4.2 and 20 K. At higher temperatures, a Hewlett Packard coupler controller (2570A) and microcomputer (HP86) were used for automatic data logging.

Temperatures below 30 K were measured with a 1000-Ω carbon resistor while above 30 K a Cu/constantan thermocouple was employed. The carbon resistor was found to be slightly field dependent below ~10 K. For measurements at other than the lowest attainable temperature (4.28 K), errors of up to 0.2 K can result from this dependence. In general, the errors in temperature were probably less than 0.1 K.

The magnetic moments of all compounds at 295 K were measured with a second Faraday balance consisting of a Newport 4-in. electromagnet and Cahn RG electrobalance. Field strengths of 5–6.5 kG, calibrated against $Hg[Co(CNS)_4]$, were used. These measurements and the Oxford Faraday measurements at 295 K generally agreed to better than 0.05 μ_B. Also, some magnetic moments at 295 K were measured by the Faraday method on a Newport Instruments Gouy balance with a $^3/_2$-in. Type C electromagnet and a Faraday kit conversion as supplied.

The diamagnetic corrections for the metal-free ligands were measured by using their hydrated bromide salts, i.e. $[sar]\cdot 4.5HBr\cdot 3H_2O$ and $[(NH_2)_2sar]\cdot 5HBr\cdot 3H_2O$. Tabulated values of Pascal's constants were used to apply corrections for HBr and H_2O giving $\chi_d[sar] = -300 \times 10^{-6}$ cm^3 mol^{-1} and $\chi_d[(NH_2)_2sar] = -172 \times 10^{-6}$ cm^3 mol^{-1}.

Results and Discussion

$3d^1$ Configuration. Although attempts to isolate cage complexes of Ti^{III} have so far been unsuccessful, two V^{IV} cages, $[V(sar\text{-}2H)](PF_6)_2\cdot 5H_2O$ and $[V((NH_3)_2sar\text{-}2H)]Cl_4\cdot 5H_2O$, have been synthesized.[7] In these cages, deprotonation at two coordinated N atoms occurs to give the first saturated N_6-donor complexes of vanadium(IV). The magnetic moments measured at 295 K, $\mu_{eff} = 1.80$ μ_B for $[V(sar\text{-}2H)]^{2+}$ and $\mu_{eff} = 1.93$ μ_B for $[V((NH_3)_2sar\text{-}2H)]^{4+}$ are consistent with the expected $3d^1$ configurations, and both show little variation when the complexes are cooled to liquid-helium temperature (e.g. Figure 2).

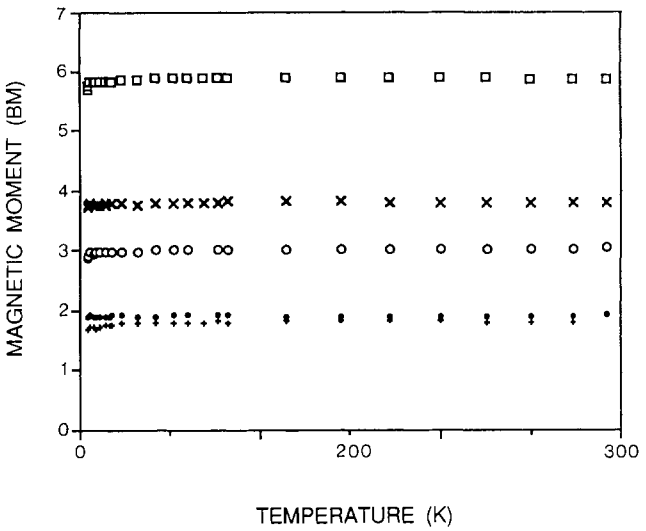

Figure 2. Magnetic moment vs temperature for $[Mn^{II}((NH_3)_2sar)](ClO_4)_4\cdot 2H_2O$ (□), $[Cr^{III}((NH_3)_2sar)]Cl_5\cdot 6H_2O$ (×), $[Ni^{II}((NH_3)_2sar)](ClO_4)_4\cdot 2H_2O$ (○), $[Cu^{II}((NH_3)_2sar)]Cl_4\cdot 2H_2O$ (●), and $[V^{IV}((NH_3)_2sar\text{-}2H)]Cl_4\cdot 5H_2O$ (+).

The marked temperature dependence of magnetic moment predicted for a $^2T_{2g}$ ground term in octahedral symmetry[9] is not observed, indicating that the VN_6 core symmetry for both complexes is lower than octahedral. An X-ray crystallographic investigation[6,7] of the complex $[V((NH_3)_2sar\text{-}2H)](S_2O_6)_2\cdot 2H_2O$ shows that the stereochemistry of the VN_6 core is close to trigonal prismatic ($\phi = 18°$) and that the two protons are absent on one strand of the ligand. Each of the two nitrogen atoms forms a trigonal-planar arrangement with the metal ion and the two adjacent carbon atoms. Thereby the $^2T_{2g}$ (O_h) term is split by a near-trigonal field to give an orbital singlet $^2A_1$ as the ground state, consistent with the near-Curie-like $\chi^{-1}(T)$ and $\mu(T)$ plots and also with EPR studies.[10]

$3d^2$ Configuration. The magnetic moment at 295 K has been measured for a V^{III} cage, prepared electrochemically from $[V((NH_3)_2sar\text{-}2H)]^{4+}$. A moment of 2.90 μ_B was obtained, consistent with the spin-only value of 2.83 μ_B expected for a d^2 ion. Similar values have been reported for $[V(en)_3]Cl_3$ (2.79 μ_B) and $[V(pn)_3]Cl_3$ (2.80 μ_B; pn = 1,2-propanediamine).[11]

The analytical and magnetic data are consistent with total protonation of the ligand occurring during the reduction of the V^{IV} complex to V^{III}. Protonation[4] of the complex is not unexpected as the pK_a's of the donor amines for the M^{III} cages are approximately 15 for Cr and Co whereas two of the coordinated N atoms for the fully protonated V^{IV} cages appear to have pK_a's less than zero.[7]

In the absence of information on both molecular structure and the temperature dependence of the magnetic susceptibility of the V^{III} cage, it can only be noted that a trigonal distortion would split the $^3T_{1g}$ (O_h) term to give either an orbital singlet, $^3A_2$ (D_3), or orbital doublet, ^3E (D_3), lying lower, either of which would be consistent with the observed moment.

The preference of six-coordinated complexes for octahedral compared with a trigonal-prismatic geometry has been analyzed[6] in terms of the dependence of d-orbital energies on the trigonal twist angle, ϕ (cf. Figure 3). If the V^{III} cage retains a similar structure to that of its V^{IV} parent with $\phi = 18°$, then a diamagnetic ground state with the electronic configuration $(a'_1)^2$ would be

(8) Mackey, D. J.; Evans, S. V.; Martin, R. L. *J. Chem. Soc., Dalton Trans.* **1976**, 1515.
(9) Machin, D. J.; Murray, K. S. *J. Chem. Soc.* **1967**, 1330.
(10) Comba, P.; Sargeson, A. M. *Aust. J. Chem.* **1986**, *39*, 1029.
(11) Clark, R. J. H.; Greenfield, M. L. *J. Chem. Soc. A* **1967**, 409.

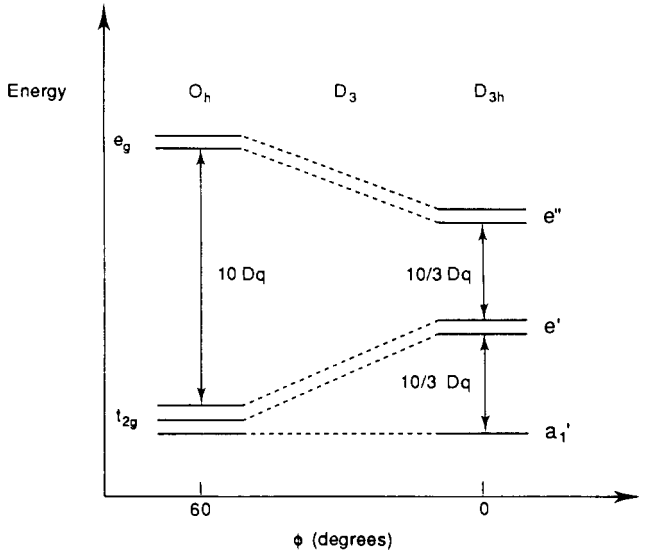

Figure 3. Variation of the energies (schematic) of the d orbitals as a function of the trigonal twist angle ϕ.

stabilized with respect to a paramagnetic state $(a'_1)^1(e')^1$ by the ligand field stabilization energy of $^{10}/_3Dq$.[12] Since the magnetism confirms an $S = 1$ ground state, it seems likely that, during reduction to V^{III} reduction, a significant increase of ϕ has occurred. A consistent value would be $\phi \sim 30°$ for a protonated $V^{III}N_6$ complex.

$3d^3$ Configuration. The magnetic moments of $[Cr(sar)](CF_3SO_3)_3$, $[Cr((NH_2)_2sar)]Cl_3\cdot H_2O$, and $[Cr((NH_3)_2sar)]Cl_5\cdot 6H_2O$ at room temperature are slightly reduced below the spin-only value of 3.87 μ_B. Similar values have been reported for other hexaamine complexes such as $[Cr(NH_3)_6]Br_3$ (3.77 μ_B),[13] $[Cr(en)_3]Br_3\cdot 3H_2O$ (3.82 μ_B),[13] and $[Cr(dtne)]Br_3$ (3.64 μ_B).[14]

Each cage complex exhibits a Curie-law $\chi^{-1}(T)$ dependence with a small decrease in μ_{eff} below $\sim$ 20 K (e.g. Figure 2). This behavior is symptomatic of a small zero-field splitting of the $^4A_{2g}$ ground term into $M_s = \pm^3/_2$ and $\pm^1/_2$ levels (separated by $2(D^2 + 3E^2)^{1/2} \approx 2D$) arising from a combination of spin–orbit coupling and ligand-field distortion effects.

A single-crystal X-ray structure[15] of $[Cr((NH_2)_2sar)]Cl_3\cdot H_2O$ shows that the CrN_6 core is close to octahedral with a trigonal twist angle $\phi = 49.0°$.[6] Accordingly, the variable-temperature magnetic data can be analyzed by using a spin Hamiltonian[16] of the type given in (1), where D and E are the axial and rhombic

$$\mathcal{H} = D[S_z^2 - {}^1/_3S(S+1)] + E[S_x^2 - S_y^2] + g\beta\mathbf{B}\cdot\mathbf{S} \quad (1)$$

zero-field-splitting parameters, $\mathbf{S}$ is the total spin operator, and $\mathbf{B}$ is the magnetic field. Good fits of the data are obtained with $g = 1.93$–1.96 and $0.5 < |D| < 1$ cm^{-1}. Inclusion of an E term did not improve the fits. The uncertainties in g and D are reasonably large because of the small variation in magnetic moment with temperature, and the sign of D cannot be evaluated from the magnetic data alone. If the g value is constrained to 1.99 in keeping with the ESR studies described below, then inferior fitting

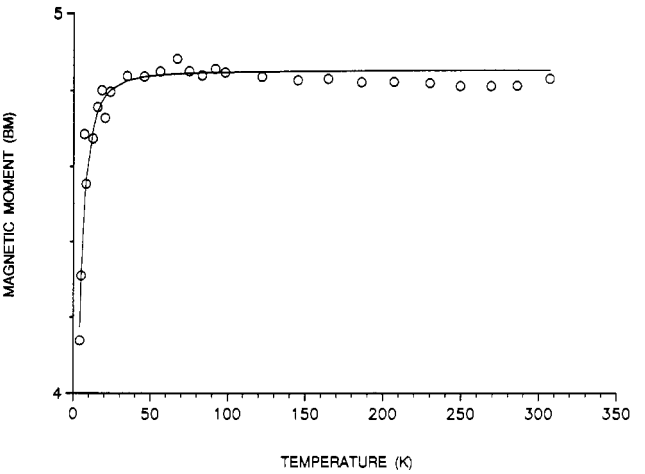

Figure 4. Magnetic moment vs temperature for $[Mn^{III}(sar)](CF_3SO_3)_3$. The solid line is the best fit to a Hamiltonian of the type shown in (1) with the parameters $S = 2$, $g = 1.98$, and $D = +5$ cm^{-1}.

of the data obtains, especially in the high-temperature region. This arises from the observed moments in this region, which are slightly below the spin-only value, e.g. for $[Cr((NH_2)_2sar)]Cl_3\cdot H_2O$, $\mu = 3.74$ μ_B at 295 K. Also, larger D values obtain. Single-crystal magnetic anisotropy and variable-field magnetization studies are required to define better the sign of D.

Well-defined ESR spectra of the Cr^{III} cages have recently been analyzed[17] with parameter values similar to those obtained here; e.g., $[Cr((NH_2)_2sar)]Cl_3\cdot H_2O$ is characterized by the parameters $g = 1.990$, $D = 0.27$ cm^{-1}, and $E = 0.04$ cm^{-1}. In this case, inclusion of a rhombic E term to the zero-field splitting was necessary to fully fit the spectrum. Distortions from axial symmetry were thought to be due to remote effects (e.g. hydrogen bonding) on the coordinated N atoms. The E term was close to zero in $[Cr((NH_3)_2sar)]Cl_5\cdot 6H_2O$, which also had a somewhat larger D value.

It is possible to estimate independently a value for the axial zero-field-splitting parameter, D, from the visible absorption spectra[15,18] of these $Cr^{(III)}$ complexes in aqueous solution. The observed splitting, δ, of the $^4A_{2g} \rightarrow {}^4T_{2g}$ band, by a small trigonal splitting, is related to D by eq 2,[19] where the spin–orbit coupling

$$|2D| \sim \frac{8\lambda^2\delta}{(10Dq)^2} \quad (2)$$

constant for Cr^{3+} is $\lambda = 90$ cm^{-1}, $\delta = 400$ cm^{-1}, and $10Dq = 22\,350$ cm^{-1} for the $[Cr((NH_2)_2sar)]^{3+}$ ion. (A positive δ indicates that the $^4A_1$ level lies below the ^4E (both levels are of origin $^4T_{2g}$ in octahedral geometry).) For these parameters, the D value obtained is 0.03 cm^{-1}, which can be compared with that deduced from the susceptibility fits and ESR spectra discussed above. The factor of 10 difference in estimates of $|D|$ obtained from these approaches is not unexpected.[19] These values can also be compared with those obtained[20] for the $[Cr(en)_3]^{3+}$ ion where $g = 1.987$, $D = 0.04$ cm^{-1} (from ESR data), and $10Dq = 21\,740$ cm^{-1}. From the above discussion, it can be seen that a spin Hamiltonian analysis of low-temperature powder susceptibility data cannot unambiguously distinguish effects of D value differences on the electronic structure of the CrN_6 chromophore. However, ESR spectroscopy does detect significant differences in D and E values that may be ascribable to remote effects rather than to distortions of the CrN_6 moiety.[17]

$3d^4$ Configuration. The temperature dependence of the magnetic moment for the manganese(III) cage $[Mn(sar)](CF_3SO_3)_3$ conforms to the behavior expected[21] for a high-spin ^5E_g ground state

(12) Wentworth, R. A. D. *Coord. Chem. Rev.* **1972/1973**, *9*, 171.
(13) Figgis, B. N.; Lewis, J. *Prog. Inorg. Chem.* **1964**, *6*, 37 and references cited therein.
(14) dtne = 1,2-bis(1,4,7-triaza-1-cyclononyl)ethane; cf.: Wieghardt, K.; Tolksdorf, I.; Herrmann, W. *Inorg. Chem.* **1985**, *24*, 1230.
(15) Comba, P.; Creaser, I. I.; Gahan, L. R.; Harrowfield, J. M.; Lawrance, G. A.; Martin, L. L.; Mau, A. W. H.; Sargeson, A. M.; Sasse, W. H. F.; Snow, M. R. *Inorg. Chem.* **1986**, *25*, 384.
(16) The computer program used on a Burroughs 6700 computer to fit this and related spin Hamiltonians for the d^4, d^5, and d^8 cases was written and developed by K. J. Berry and called COM/MAG. It involves diagonalization of the appropriate matrix under the spin Hamiltonian operator. The individual x, y, and z components of susceptibility are calculated and then averaged to give χ (average). The program employs the thermodynamic expression for susceptibility rather than Van Vleck's equation. For further details, see: Berry, K. J.; Clark, P. E.; Murray, K. S.; Raston, C. L.; White, A. H. *Inorg. Chem.* **1983**, *22*, 3928.
(17) Strach, S. J.; Bramley, R. *J. Chem. Phys.* **1988**, *88*, 7380.
(18) Comba, P.; Martin, L. L.; Sargeson, A. M. Manuscript in preparation.
(19) Wertz, J. E.; Bolton, J. R. *Electron Spin Resonance*; McGraw-Hill: New York, 1972.
(20) McGarvey, B. R. *J. Chem. Phys.* **1964**, *41*, 3743.
(21) Kennedy, B. J.; Murray, K. S. *Inorg. Chem.* **1985**, *24*, 1552.

(Figure 4). The magnetic moment is essentially independent of temperature in the range 20–300 K, the observed value of 4.83 ± 0.03 μ_B being slightly below the spin-only value. The magnetic moment below 20 K falls steadily until a value of 4.14 μ_B is reached at 4.2 K, indicative of the presence of zero-field splitting.

The combined effect of noncubic symmetry and/or Jahn–Teller distortion removes the orbital degeneracy of the ^5E_g ground term to give an orbital singlet lowest approximating to either $^5A_{1g}$ or $^5B_{1g}$ (in D_{4h} symmetry). The spin degeneracy of the ground state is lifted by spin-orbit coupling to give $M_s = 0, \pm 1$ (separated by D), and ±2 levels (separated by $3D$) with the nature of the ground level depending critically on the symmetry of the ligand field about the Mn^{III} central ion. The magnetic data conform well to a $S = 2$ spin Hamiltonian of the type shown in (1), with $g = 1.98 \pm 0.01$ and $D = 5 \pm 0.5$ cm^{-1}. Variable-field magnetization studies would be required to define better the sign and size of D and hence the exact nature of the ground state.

The single-crystal X-ray structure determination[22] for $[Mn(sar)](NO_3)_3$ reveals distortion from octahedral symmetry with a twist angle[23] of $\phi = 27°$ and three different Mn–N distances of 2.177 (11), 2.082 (10), and 2.129 (10) Å. This is consistent with splitting of the ^5E_g (O_h) state and hence with the magnetic data, assuming that the NO_3^- and $CF_3SO_3^-$ salts have the same Mn^{III} stereochemistry.

The published chemistry of manganese(III) with six nitrogen ligands is still quite limited. The only reference to a tris-bidentate species is to $[Mn(en)_3](ClO_4)_3$, which is reported to be a green crystalline compound with $\mu_{eff} = 4.85$ μ_B and $g = 2.08$.[24]

3d^5 Configuration. Examples of both high-spin ($t_{2g}^3e_g^2$), and low-spin (t_{2g}^5) ground states have been observed for d^5 cages containing Mn^{II} and Fe^{III}. Their bulk susceptibilities have been measured over the temperature range 4.2–300 K and are discussed below according to the spin multiplicity of the ground state.

(i) High-Spin d^5 Configuration. The magnetic susceptibilities of two Mn^{II} complexes have been measured over the above temperature range and both complexes, $[Mn(sar)](ClO_4)_2$ and $[Mn((NH_3)_2sar)](ClO_4)_4 \cdot 2H_2O$, are high-spin; i.e., $S = {}^5/_2$. The reciprocal magnetic susceptibilities of both complexes vary linearly with the temperature. The magnetic moments are close to the spin-only value at 300 K (5.91 and 5.85 μ_B, respectively) and only decrease significantly at temperatures below about 20 K reaching 5.70 μ_B at 4.2 K for both complexes (e.g. Figure 2).

This small decrease in moment observed at low temperatures is attributed to the combined action of second-order spin–orbit coupling and lowering of the symmetry below octahedral. The magnetic properties in this low-temperature region have been reproduced by using a $S = {}^5/_2$ spin Hamiltonian of the type shown in (1), with $g = 2.00 \pm 0.01$ and $|D| = 0.5 \pm 0.1$ cm^{-1}. Inclusion of a rhombic (E) term into the calculation did not significantly improve the fit.[16] Zero-field splitting parameters of similar magnitude were also deduced from the 4.2 K ESR spectra,[25] with $D = 0.19$ cm^{-1} and $E = 0.0063$ cm^{-1} for $[Mn(sar)]^{2+}$ and $D = 0.18$ cm^{-1} and $E = 0.012$ cm^{-1} for $[Mn((NH_3)_2sar)]^{4+}$.

The high-spin behavior of the two manganese cages parallels closely the magnetism reported for other saturated amine complexes, such as $[Mn(NH_3)_6]CrO_4$,[26] $[Mn(en)_3]Br_2$,[27] and $[Mn(dtne)](PF_6)_2$.[14]

(ii) The Low-Spin d^5 Configuration. The Fe^{3+} ion, with its higher charge compared to the Mn^{2+} ion, is expected to experience a significantly stronger ligand field. Thus the low-spin magnetic behavior found for the $[Fe(sar)]Cl_3 \cdot H_2O$ complex is not unexpected and has been observed previously with other saturated amine complexes.[14,28,29]

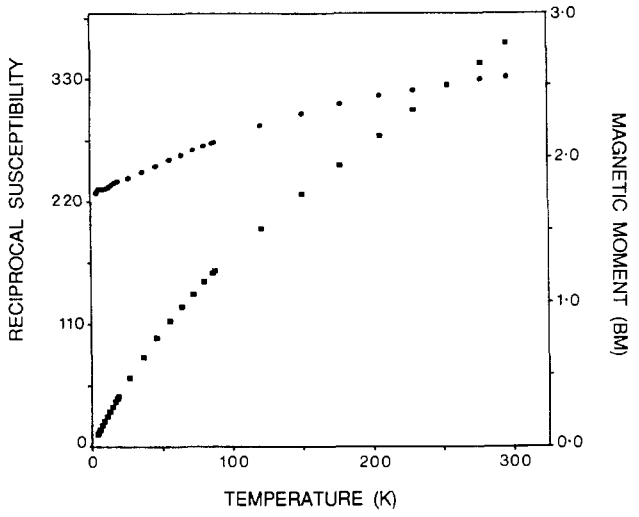

Figure 5. Magnetic moment (●) and reciprocal susceptibility (■) vs temperature for $[Fe^{III}(sar)]Cl_3 \cdot H_2O$.

The magnetic moment at 295 K of 2.55 μ_B for $[Fe(sar)]Cl_3 \cdot H_2O$, confirms the presence of a significant orbital contribution ($\mu_{so} = 1.73$ μ_B). However, as the temperature is lowered, the moment decreases towards the spin-only value as expected (Figure 5). The graph of reciprocal molar susceptibility vs temperature (Figure 5) follows the Curie law only below ~40 K and exhibits substantial deviation from linearity at higher temperatures.

The 3-fold orbital degeneracy of the $^2T_{2g}$ ground term can be lifted either by axial distortion or spin–orbit coupling or a combination of both. The susceptibility data for $[Fe(sar)]Cl_3 \cdot H_2O$ were analyzed by using a program called COM/LSYM,[30] where the axial splitting parameter, δ_{ax}, and the spin–orbit coupling constant, λ, were both allowed to vary. The parameters of best fit are $\delta_{ax} = 400 \pm 100$ cm^{-1} and $\lambda = -300 \pm 50$ cm^{-1} (free ion value −460 cm^{-1}). Similar values have been estimated for other low-spin iron(III) amine complexes.[29,31] The ESR spectrum[25] of $[Fe(sar)]Cl_3 \cdot H_2O$ shows signals at $g_\parallel = 2.93$ and $g_\perp = 2.12$, from which a δ_{ax} value of 120 cm^{-1} was deduced (for $\lambda = -460$ cm^{-1}), which is in fair agreement with the present value.

The small splitting of the ligand field is consistent with the X-ray structure determination of $[Fe(sar)](NO_3)_3$, where ϕ deviates only 7° from ideal octahedral symmetry.[6]

3d^6 Configuration. A large number of cobalt(III) cages have been characterized and all are low-spin as deduced from their electronic and ^1H NMR spectra and structural properties.[2,4,6]

In contrast, the iron(II) cages exhibit either high-spin or low-spin d^6 configurations depending on the nature of the apical substituents.[4] It follows that the ligand-field generated by the cage must place iron(II) close to its electronic spin crossover, and thus it was not unexpected that these complexes exhibit a temperature-dependent low-spin ⇄ high-spin equilibrium in solution.[4,32]

The $[Fe(sar)]^{2+}$ and $[Fe((NH_3)_2sar)]^{4+}$ complexes are air-sensitive and oxidize readily to give imines. However, strict anaerobic conditions allow imine-free samples to be prepared.

(i) The High-Spin d^6 Configuration. Both $[Fe((NH_3)_2sar)]Cl_2Br_2 \cdot 4H_2O$ and $[Fe(sar)](CF_3SO_3)_2$ have high-spin $t_{2g}^4e_g^2$ configurations giving rise to ground states of $^5T_{2g}$ origin in octahedral geometry. Variations of magnetic moment with temperature of 5.42→4.44 μ_B (230→4.2 K) and 5.15→3.82 μ_B (230→4.2 K) were observed, respectively. The value for the

(22) Martin, L. L.; Snow, M. R.; Tiekink, E.; Sargeson, A. M. Submitted for publication.
(23) Tiekink, E. Personal communication.
(24) Summers, J. C. *Diss. Abstr. Int.* **1969**, *B30*, 109. See also: *Gmelin's Handbook of Inorganic Chemistry*; Springer-Verlag: West Berlin, 1982; Vol. D3, p 42.
(25) Comba, P. Unpublished data.
(26) Narain, G.; Shukla, P. *J. Indian Chem. Soc.* **1966**, *43*, 694.
(27) Watt, G. W.; Manhas, B. S. *J. Inorg. Nucl. Chem.* **1966**, *28*, 1945.
(28) Wieghardt, K.; Schmidt, W.; Herrmann, W.; Küppers, H.-J. *Inorg. Chem.* **1983**, *22*, 2953.
(29) Renovitch, G. A.; Baker, W. A. *J. Am. Chem. Soc.* **1968**, *90*, 3585.
(30) This computer program is similar to the other COM/MAG program in ref 16 and has been described for t_{2g}^5 systems in: Gunter, M. J.; Berry, K. J.; Murray, K. S. *J. Am. Chem. Soc.* **1984**, *106*, 4227.
(31) Figgis, B. N. *Faraday Soc. Trans.* **1961**, *57*, 204.
(32) Martin, L. L.; Hagen, K.; Hauser, A.; Martin, R. L.; Sargeson, A. M. *J. Chem. Soc., Chem. Commun.* **1988**, 1313.

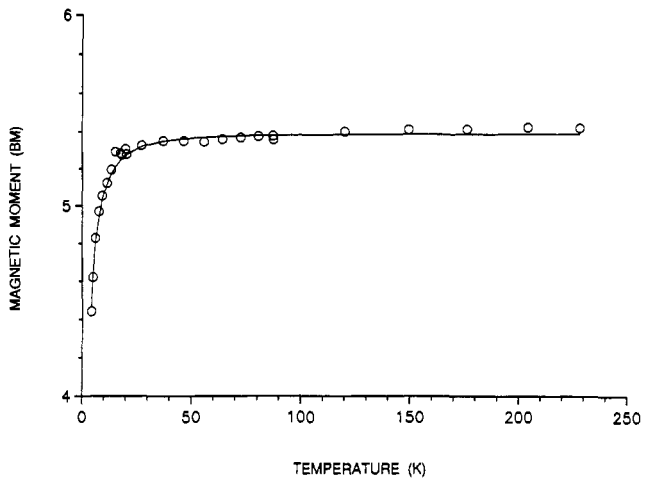

Figure 6. Magnetic moment vs temperature for $[Fe^{II}((NH_3)_2sar)]Cl_2Br_2 \cdot 4H_2O$. The solid line is the best fit to a Hamiltonian of the type shown in (1) with the parameters $S = 2$, $g = 2.2$, and $D = 6.8$ cm^{-1}.

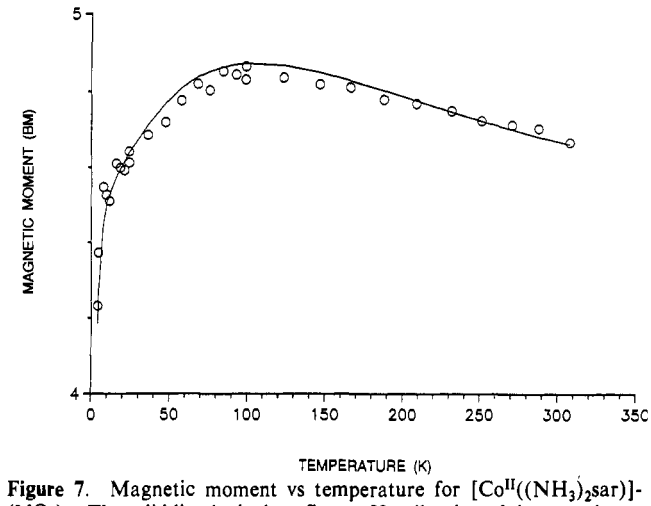

Figure 7. Magnetic moment vs temperature for $[Co^{II}((NH_3)_2sar)](NO_3)_4$. The solid line is the best fit to a Hamiltonian of the type shown in (3) with the parameters $S = {}^3/_2$, $\lambda = -100$ cm^{-1}, $k = 1$, $R = 0$, and $\Delta = -9000$ cm^{-1}.

moment at the highest attainable temperature lies above the spin-only value of 4.90 μ_B due to orbital degeneracy of the ground state.

An X-ray structural analysis for $[Fe((NH_3)_2sar)](NO_3)_4 \cdot H_2O$ shows a distortion of essentially a D_3 molecule with an intermediate trigonal twist angle,[6] $\phi = 29°$, and variations in the Fe–N bond distances[33] (2.18–2.24 Å) are observed. Such distortions cause a splitting of the $^5T_{2g}$ parent state into an orbital singlet ground state, a situation compatible with the magnetic behavior. The effective magnetic moment for $[Fe((NH_3)_2sar)]^{4+}$ is insensitive to temperature from 230 to 40 K (Figure 6), below which the moment falls by ~ 1 μ_B (40→4.2 K), to a value below the spin-only moment. This type of $\mu(T)$ dependence is indicative of zero-field splitting of the orbital singlet with a nonmagnetic sublevel (i.e. $M_s = 0$) lying lowest.

An excellent fit can be obtained using the $S = 2$ spin Hamiltonian (1) with the parameters $g = 2.2 \pm 0.01$ and $D = 6.8 \pm 0.1$ cm^{-1} (Figure 6). The D value is large in this case because spin–orbit coupling connects the ground singlet with the other component of the $^5T_{2g}$ state. Since the parent $^5T_{2g}$ state is orbitally degenerate, an appropriate Hamiltonian of the type given in (3)

$$\mathcal{H} = -\lambda \mathbf{LS} + (\Delta/9)[3L_z^2 - L(L+1)] + (R/12)[L_+^2 + L_-^2] + \beta \mathbf{B}(k\mathbf{L} + 2\mathbf{S}) \quad (3)$$

was also employed, where Δ and R are axial and rhombic splitting parameters and k is the orbital reduction factor.[34] Use of very large values of Δ and R make this model similar to the ZFS Hamiltonian (1) but no notable improvement in fit was obtained compared to the use of (1).

The magnetic properties of several salts of $[Fe(en)_3]^{2+}$ lie in the range μ (291 K) = 5.13–5.39 μ_B; however, the temperature dependence differs for each salt.[35]

(ii) The Low-Spin d^6 Configuration. $[Fe((NH_2)_2sar)](CF_3SO_3)_2$ is deep blue with strong electronic transitions in the visible region, indicating that its magnetic behavior should differ from the above colorless high-spin Fe^{II} cages. Indeed, the susceptibility measured at room temperature was negative, confirming a low-spin configuration and a $^1A_{1g}$ ground state in octahedral geometry. Clearly, lattice forces within the crystal must play a significant role in determining the nature of the ground state as dissolution of each of the Fe^{II} cages resulted in a spin equilibrium between states of origin $^1A_{1g}$ and $^5T_{2g}$.[4,32]

Another pseudooctahedral, saturated Fe^{II} amine complex that must lie extremely close to the spin crossover is $[Fe([9]aneN_3)_2]^{2+}$.[36] In this case, an anion dependence is observed for polycrystalline samples, with the dibromide tetrahydrate being diamagnetic, yet removal of the water of crystallization under vacuum yields a paramagnetic material with a temperature dependence of its moment.[28,36]

3d^7 Configuration. The magnetic properties of the 3d^7 configuration depend on whether the ground state is high-spin ($^4T_{1g}$) or low-spin (^2E_g) in the octahedral ligand field. The temperature dependence of the magnetic susceptibility (4–300 K) was measured for five cobalt(II) cage complexes and one nickel(III) cage complex having the N_6 donor core but only the last was low spin. In addition, the influence of the donor atoms has been examined by measuring the magnetic properties of a $Co^{II}N_3S_3$ cage.

(i) The High-Spin 3d^7 Configuration. The five high-spin complexes studied were $[Co(sar)](ZnCl_4)$, $[Co((NH_3)_2sar)](ZnCl_4)_2$, $[Co((NH_3)_2sar)]Cl_4 \cdot H_2O$, $[Co((NH_3)_2sar)](NO_3)_4$, and Δ-(*lel*)$_3$-$[Co((NO_2)_2char)](ClO_4)_2 \cdot 2H_2O$.[37,38]

The Co^{II} cages are readily oxidized to the Co^{III} diamagnetic state by O_2. Therefore, the magnetic purity of the $[Co((NH_3)_2sar)]^{4+}$ complexes was established from the reproducibility of $\chi(T)$ for four different anions. The chloride and zinc tetrachloride salts gave similar results with μ_{eff}(300 K) ≈ 4.5 μ_B, typical of a high-spin d^7 system with a ground term of origin $^4T_{1g}$. Both complexes showed an increase in the magnetic moment as the temperature was lowered below 300 K, reaching a maximum value of about 4.6 μ_B at ~ 100 K, below which μ_{eff} decreased as the temperature was lowered further. The moments at 295 K of ca. 4.5 μ_B lie above the spin-only value of 3.87 μ_B due to a significant orbital contribution to the moment. The $^4T_{1g}$ ground term and the usual value of the spin–orbit coupling constant for the Co^{II} ion, $\lambda = -170$ cm^{-1}, results in a calculated magnetic moment of about 5.1 μ_B (at 300 K). The somewhat reduced value observed can be attributed to a symmetry lower than octahedral for the Co^{II} cage complexes. Indeed, the X-ray crystal structure reported for $[Co((NH_3)_2sar)](NO_3)_4 \cdot H_2O$, confirms the presence of a significant trigonal distortion of the CoN_6 core from octahedral symmetry, with a trigonal twist angle of $\phi = 29°$.[6]

The magnetic moment of the nitrate salt of $[Co((NH_3)_2sar)]^{4+}$ varied in a similar manner to that of the chloride and tetrachlorozincate salts over the same temperature range (Figure 7). However, the curve is displaced slightly to higher moments with a room temperature moment of 4.70 μ_B rising to 4.86 μ_B (at ~ 100

(33) Creaser, I. I.; Hagen, K. S.; Martin, L. L.; Sargeson, A. M.; White, A. H. Unpublished data.
(34) Bohan, T. L. *J. Magn. Reson.* **1977**, *26*, 109.
(35) Renovitch, G. A. Ph.D. Thesis, Syracuse University, 1969.
(36) ([9]aneN$_3$) = 1,4,7-triazacyclononane; cf.: Wieghardt, K.; Küppers, H. J.; Weiss, J. *Inorg. Chem.* **1985**, *24*, 3067.
(37) $(NO_2)_2$char = 1,12-dinitro-3,10,14,21,24,31-hexaazapentacyclo-[10.10.10.0.0.0]dotriacontane; cf.: Geue, R. J.; McCarthy, M. G.; Sargeson, A. M. *J. Am. Chem. Soc.* **1984**, *106*, 8282.
(38) *ob* and *lel* nomenclature refers to the conformers where the alignment of the C–C bond for the ethylenediamine chelate rings is oblique or parallel to the C_3 axis of the octahedral complex. See: *Inorg. Chem.* **1970**, *9*, 1.

Table I. Ligand-Field Parameters for Pseudooctahedral Ni^{II} Complexes with σ-Donor Ligands (cm^{-1})

ligand	Dq	$B_{35} \sim B_{55}$	β	B_{33}	ref
NH_3	1080	890	0.85_5		53
en	1160	840	0.81		53
sar	1243	860	0.82_5	733	4, 18
$(NH_3)_2$sar	1242	858	0.82_5	728	4, 18
9-aneN_3	1260	860	0.82_5	730	41

K) and then falling to 4.23 μ_B (at 4.2 K). The $\mu(T)$ curve for a second preparation of the tetrachloride salt exhibited the same overall shape; however, at 240 K, μ_{eff} = 4.83 μ_B, which dropped to μ_{eff} = 4.46 μ_B at 4.2 K.

The magnetic behavior of the $[Co^{II}(sar)](ZnCl_4)$ complex also conforms well with that observed for the $[Co((NH_3)_2sar)]^{4+}$ complexes (chloride, nitrate, and tetrachlorozincate salts) with μ_{eff}(215 K) = 4.42 μ_B decreasing to μ_{eff} = 3.82 μ_B at 4.2 K. (Instrumental difficulties restricted the measurement of moments above 215 K.)

The above data confirm that although the overall shapes of the $\mu(T)$ curves are very similar, minor variations in moment values of the order of ± 0.1 μ_B do occur depending on both the nature of the anion and/or small differences in the preparative procedures.

The $\Delta(lel)_3$-$[Co((NO_2)_2char)](ClO_4)_2 \cdot 2H_2O$ complex[37,38] was also studied to extend the range of Co^{II} cages. At room temperature $\Delta(lel)_3$-$[Co((NO_2)_2char)](ClO_4)_2 \cdot 2H_2O$ exhibits a magnetic moment μ_{eff} = 4.73 μ_B, which increases to 4.80 μ_B as the temperature is lowered to ~140 K and then falls to 4.16 μ_B at 4.2 K. This behavior is almost identical with that observed for $[Co((NH_3)_2sar)](NO_3)_4$ as illustrated in Figure 7. Clearly the electron-withdrawing nature of the apical substituents and structural variations caused by the conformational rigidity of the cyclohexane rings have little effect on the magnetic properties.

Attempts were made to fit the high-spin data by using a parametric model[39] that included the simultaneous perturbation by both spin–orbit coupling and ligand-field distortions. Unfortunately, it was not possible to obtain an unambiguous choice of parameters. By the use of a Hamiltonian of the type shown in (3), the best fit[39] was obtained with $\lambda = -100$ cm^{-1}, $k = 1$, $R = 0$, and $\Delta = -9000$ cm^{-1} (Figure 7). However, good fits could be obtained for a range of Δ values from −3000 to −9000 cm^{-1}, indicating that an orbital doublet lies lowest but that the magnetic data are quite insensitive to this parameter. In fact, the inherent difficulty of interpreting $\chi(T)$ behavior for the cobalt(II) ion is well-documented in several reviews,[13,40] which include many examples of magnetically dilute octahedral Co^{II} complexes with room-temperature moments ranging from 4.25 to 5.4 μ_B. This "large spread" of values is attributed (in part, at least) to distortions that influence the magnitude of the splitting of the $^4T_{1g}$ ground term and thereby reduce the orbital contribution to the observed magnetic moment.

Although considerable diversity has been found in the magnetic moment values and temperature dependences for the Co^{II} cages, they are generally compatible with the behavior expected for a trigonally distorted octahedral geometry. The ESR spectrum of $[Co((NH_3)_2sar)]^{4+}$ in DMSO solution[25] shows well-resolved lines, and the deduced parameters of $g_x = 2.039$, $g_y = 4.837$ and $g_z = 4.328$ are also typical of a distorted octahedral geometry.[40]

The visible spectrum[4,18] of $[Co((NH_3)_2sar)]^{4+}$ has characteristic bands at 10 320 cm^{-1} ($^4T_{1g} \rightarrow {}^4T_{2g}(F)$) and 21 220 cm^{-1} ($^4T_{1g} \rightarrow {}^4T_{1g}(P)$) from which the deduced (ignoring spin–orbit splitting of the ground state) ligand-field parameters are $10Dq \cong 11\,570$ cm^{-1} and $B = 800$ cm^{-1} (with $B_0 = 970$ cm^{-1} and $\beta = 0.82_5$), consistent with the values for Ni^{II} (Table I). These parameters are very similar to those reported[41] ($10Dq = 12\,000$ cm^{-1}, $B =$ 780 cm^{-1}, and $\beta = 0.82_5$) for the corresponding triazacyclononane complex $[Co(9\text{-ane}N_3)_2]I_2 \cdot 2H_2O$ which is also high spin.

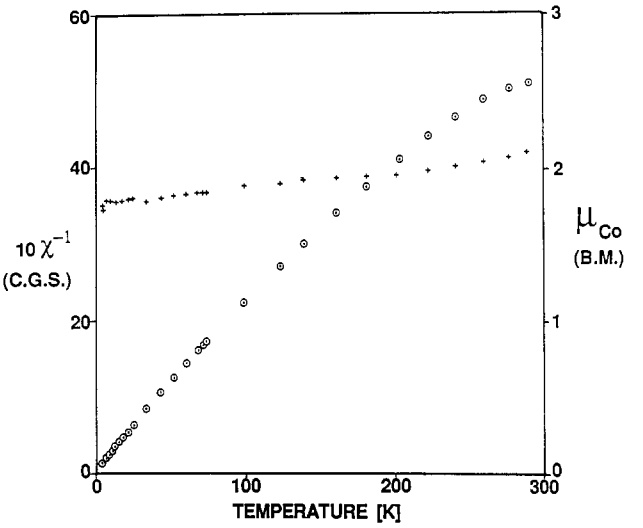

Figure 8. Magnetic moment (+) and reciprocal susceptibility (⊙) vs temperature for $[Co^{II}((aza)capten)](CF_3SO_3)_2$.

(ii) The Low-Spin d^7 Configuration. A change in donor atoms from N_6 to N_3S_3 is associated with a change in spin state for cobalt(II) cage complexes. Thus the $[Co(sar)]^{2+}$ and $[Co((NH_3)_2sar)]^{4+}$ cages are high-spin whereas the trithia complex $[Co((aza)capten)]^{2+}$ has a low-spin ground state. This is not unexpected because the above ligand field parameters for the N_6 cages indicate that the low-spin ^2E_g term lies only a few thousand wavenumbers above the ground state. The energy of the low-spin ^2E_g (t_2^6e) term with respect to the ground $^4T_{1g}$ ($t_2^5e^2$) state is given[42] by $4B + 4C - 10Dq \cong 5500$ cm^{-1} although this estimate is only approximate because configuration interaction between the two $^4T_{1g}$ terms and between the five ^2E_g states as well as spin–orbit coupling are not taken into account ($C/B = 4.3_5$).[41]

The magnetic behavior of the complex $[Co((aza)capten)](CF_3SO_3)_2$[43] was included in this study in order to observe the influence of sulfur donor atoms on the temperature dependence of the magnetism within a similar cagelike environment. The magnetic moment was remeasured; μ_{eff}(289 K) = 2.12 μ_B, compared to an earlier value at room temperature of μ_{eff}(298 K) = 1.89 μ_B.[43] Over the temperature range 289–4.2 K, the moment decreases from 2.12 μ_B to the spin-only value of 1.73 μ_B (Figure 8), consistent with a low-spin t_2^6e ground state. The slight increase in the μ_{eff} at high temperatures and the corresponding curvature in $\chi^{-1}(T)$ probably indicates the presence of low-lying $^4T_1$ states, a feature observed in other low-spin cobalt(II) chelates[44] and consistent with the small high-spin–low-spin energy separation estimated above.

Encapsulation of the nickel(III) ion by the sar ligand provided an opportunity to examine the low-spin d^7 configuration with the N_6 donor ligand. The temperature dependence of the magnetic moment of $[Ni(sar)](CF_3SO_3)_3$ falls monotonically from 1.97 μ_B (at 307 K) to 1.75 μ_B (at 4.2 K). The low-spin character of the $[Ni(sar)]^{3+}$ ion contrasts with the high-spin $[Co(sar)]^{2+}$ ion character and reflects the influence on $10Dq$ and B of the higher charge of the nickel(III) ion.

ESR measurements confirm the low-spin magnetism of $[Ni(sar)]^{3+}$ and, in addition, reveal anisotropy in the g values. For powder samples at 4.2 K, two g values of 2.113 and 2.04 were obtained with indications of a small rhombic splitting fo the g =

(39) Two separate computer programs were used in sequence to fit these data. Both these programs were written by E. N. Bakshi and run on a VAX/VMS computer. (1) MATRIX produced the matrix elements for the appropriate Hamiltonian, and (2) MAGB employed the above matrix elements to calculate the magnetic susceptibility.

(40) Banci, L.; Bencini, A.; Benelli, C.; Gatteschi, D.; Zanchini, C. *Struct. Bonding* **1982**, *52*, 37.

(41) Reinen, D.; Ozarowski, A.; Jakob, B.; Pebler, J.; Stratemeier, H.; Wieghardt, K.; Tolksdorf, I. *Inorg. Chem.* **1987**, *26*, 4010.

(42) Jørgensen, C. K. *Absorption Spectra and Chemical Bonding in Complexes*; Pergamon Press: Oxford, England, 1962.

(43) (aza)capten = (1-methyl-3,13,16-trithia-6,8,10,19-tetraazabicyclo-[6.6.6]icosane); cf.: Gahan, L. R.; Hambley, T. W.; Sargeson, A. M.; Snow, M. R. *Inorg. Chem.* **1982**, *21*, 2699. Dubs, R. V.; Gahan, L. R.; Sargeson, A. M. *Inorg. Chem.* **1983**, *22*, 2523.

(44) Murray, K. S.; Sheahan, R. M. *J. Chem. Soc., Dalton Trans.* **1976**, 999.

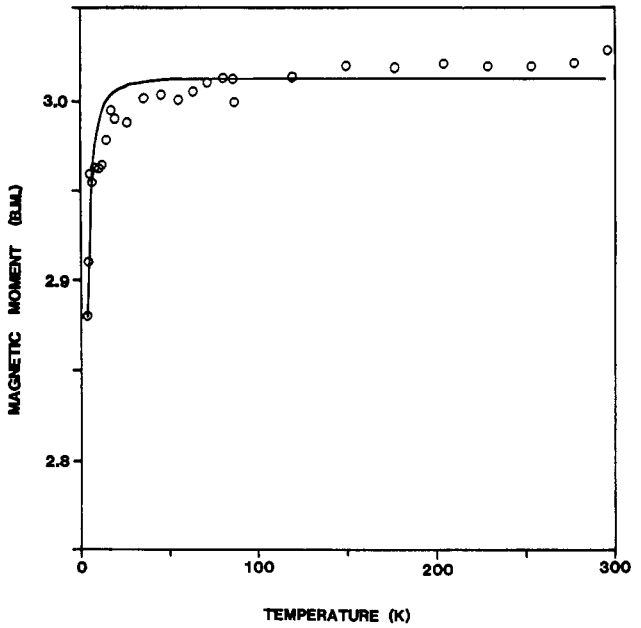

Figure 9. Magnetic moment vs temperature for $[Ni^{II}((NH_3)_2sar)](ClO_4)_4 \cdot 2H_2O$. Data were fitted to a Hamiltonian of the type shown in (1) with the parameters $S = 1$, $g = 2.13$, and $D = 1.7$ cm^{-1}.

2.04 line.[25] The total line shape implies that the unpaired electron resides in an orbital chiefly d_{z^2} in character, i.e. a $^2A_{1g}$ (D_{4h}) ground state, although single-crystal measurements would be required to assign unambiguously the ground state.

The lack of available low-spin hexaamine complexes for comparison is not unexpected since the isolation of stable nickel(III) complexes is still rare and their magnetic characterization is even more elusive. However, the report[28] of another hexaamine complex, $[Ni([9]aneN_3)_2](ClO_4)_3$, with a moment of 2.0 μ_B at 293 K agrees well with the observed behavior of the present nickel(III) cage. The ESR spectrum of the $S_2O_6^{2-}$ salt of this complex is also very similar to that of $[Ni(sar)]^{3+}$, and a $^2A_{1g}$ ground state was confirmed by single-crystal measurements on this tetragonally elongated octahedral system.[45]

3d^8 Configuration. The magnetic properties of the cage complexes $[Ni((NH_3)_2sar)](ClO_4)_4 \cdot 2H_2O$ and $[Ni(sar)](ClO_4)_2$ conform to those expected for a $^3A_{2g}$ ground state in pseudooctahedral symmetry. The magnetic moments at 300 K are 3.03 and 3.06 μ_B, respectively, the susceptibilities following a Curie–Weiss law with small values of $\Theta = 1.5$ K.

The 3-fold spin degeneracy of the ground term is lifted by spin–orbit coupling to give a small zero-field splitting, D, which results in a reduction in μ_{eff} at temperatures below about 25 K (Figure 2). Analysis of the data using the Hamiltonian (1) for $S = 1$ yields a good fit over the temperature range 4.2–300 K with $g = 2.13 \pm 0.01$ and $|D| = 1.7 \pm 0.1$ cm^{-1} (Figure 9).

The zero-field splitting parameter can be estimated independently[19] from the optical absorption spectrum of $[Ni((NH_3)_2sar)]^{4+}$

$$D = \zeta^2[1/E(^3B_{2g}) - 1/E(^3E_g)] \quad (4)$$

where ζ is the one-electron spin–orbit coupling constant for Ni^{2+} ($\lambda = \zeta/2S$) and $E(^3E_g)$ and $E(^3B_{2g})$ are the energies of the electronic excitations $^3A_{2g} \rightarrow {}^3B_{2g}$ ($^3T_{2g}$) (11 390 cm^{-1}) and $^3A_{2g} \rightarrow {}^3E_g$ ($^3T_{2g}$) (12 420 cm^{-1}) assuming a tetragonal[18] (or a trigonal) field. Employing a value of ζ of 500 cm^{-1} (free ion value is 630 cm^{-1}) leads to $D \approx +2$ cm^{-1}, which is in good agreement with the value derived from the magnetic data. In making this analysis, we note that controversy exists in the literature as to the origin for the splitting of the first ligand-field band often observed for octahedral nickel(II) complexes. It has been argued that the splitting of the $^3A_{2g} \rightarrow {}^3T_{2g}$ transition by low-symmetry components is incorrect[46,47] and that a more correct assignment arises from mixing of this transition with that of $^3A_{2g} \rightarrow {}^1E_g$ character.

Both the nitrate and chloride salts of $[Ni((NH_3)_2sar)]^{4+}$ have been studied by X-ray methods.[48] The Ni–N bond lengths in the nitrate salt are essentially equal (2.11 ± 0.01 Å)[6] whereas, in the chloride salt, two Ni–N bonds (2.08 ± 0.01 Å) are marginally shorter than the other four (2.12 ± 0.01 Å). These differences arise from different conformations of the chelate rings; $(lel)_2(ob)$ for the chloride and $(lel)_3$ for the nitrate salt.[38] However, the observed trigonal twist angles for the two complexes are close, with $\phi = 46 \pm 1°$.[6]

The magnetic properties of the parent ethylenediamine complex[8] $[Ni(en)_3](NO_3)_2$ are very similar with $\mu_{eff} = 3.08 \pm 0.02$ μ_B (30–300 K), and which falls to 2.2 μ_B as the temperature is lowered from 30 to 4.2 K. The zero-field-splitting parameter was calculated to be $D = -0.65$ cm^{-1}. Crystallographic data indicate that the NiN_6 core is distorted from octahedral symmetry by both compression along the 3-fold axis and a twist toward trigonal prismatic coordination.[8]

3d^9 Configuration. The temperature dependence of the magnetic susceptibility of $[Cu((NH_3)_2sar)]Cl_4 \cdot 6H_2O$ and $[Cu(sar)](ClO_4)_2$ follows the Curie–Weiss law with small values of Θ (0.1 and 0.9 K, respectively). The magnetic moments at 300 K are 1.92 and 1.91 μ_B (decreasing to 1.89 and 1.79 μ_B at 4.3 K) (e.g. Figure 2), similar to that reported for $[Cu(en)_3]SO_4$ of 1.86 μ_B.[49]

The X-ray crystal structure of $[Cu((NH_3)_2sar)]Cl_4 \cdot 6H_2O$ reveals that there are three different Cu–N bond lengths (2.046, 2.160, and 2.290 Å), confirming that the combination of Jahn–Teller and ligand conformational effects lower the molecular symmetry.[48] The ESR spectra in frozen solutions of $[Cu((NH_3)_2sar)]^{4+}$ and $[Cu(sar)]^{2+}$ exhibit three g values characteristic of a tetragonal plus rhombic ligand field; e.g. for $[Cu((NH_3)_2sar)]^{4+}$, $g_x = 2.04$, $g_y = 2.069$, and $g_z = 2.22$,[25] similar to those observed for $[Cu(en)_3]^{2+}$, $g_x = 2.053$, $g_y = 2.134$ and $g_z = 2.159$,[25] which has a symmetry lower than trigonal,[50] and for $[Cu([9]aneN_3)_2]^{2+}$, which has a tetragonally elongated octahedral geometry in which the in-plane Cu–N distances are nearly equal.[51] These data are consistent with an orbital singlet ground state $^2B_{1g}$ (D_{4h}, vacancy in $d_{x^2-y^2}$) into which excited states are mixed by spin–orbit coupling to give a predicted magnetic moment of about 1.9 μ_B, which should remain nearly independent of temperature.

3d^{10} Configuration. The zinc(II) complexes $[Zn(sar)](CF_3SO_3)_2$ and $[Zn((NH_3)_2sar)](CF_3SO_3)_4$ were studied at room temperature, and both complexes proved to be diamagnetic as expected with uncorrected χ_M values of -8.13×10^{-5} and -4.14×10^{-4} cm^3 mol^{-1}, respectively. These results also indicate that the free cages from which the complexes were synthesized are free of contamination by paramagnetic ions.

Conclusions

It is unusual to have available a series of complexes with the same ligancy that encompasses almost all members of the first-row transition-metal ions from V to Zn. Moreover, the encapsulating coordination environment enables the magnetic properties of the metal ion to be studied in a magnetically dilute situation for 3d$^{1-10}$ electron configurations, usually in two oxidation states. It was therefore especially desirable for this systematic study to be carried out.

The metal(II) cage complexes of $[M(sar)]^{2+}$ and $[M((NH_3)_2sar)]^{4+}$ with the exception of $[Fe((NH_2)_2sar)](CF_3SO_3)_2$

(45) Wieghardt, K.; Walz, W.; Nuber, B.; Weiss, J.; Ozarowski, A.; Stratemeier, H.; Reinen, D. *Inorg. Chem.* **1986**, *25*, 1650.
(46) Hart, S. M.; Boeyens, J. C. A.; Hancock, R. D. *Inorg. Chem.* **1983**, *22*, 982.
(47) Jørgensen, C. K. *Acta Chem. Scand.* **1955**, *9*, 1362.
(48) Creaser, I. I.; Harrowfield, J. M.; Martin, L. L.; Sargeson, A. M.; White, A. H. Submitted for publication.
(49) Mitra, S. N.; Sengupta, P. *Indian J. Phys.* **1973**, *47*, 79.
(50) Bertini, I.; Gatteschi, D.; Scozzafova, A. *Inorg. Chim. Acta* **1974**, *11*, L17.
(51) Chaudhuri, P.; Oder, K.; Wieghardt, K.; Weiss, J.; Reedijk, J.; Hinrichs, W.; Wood, J.; Ozarowski, A.; Stratemeier, H.; Reinen, D. *Inorg. Chem.* **1986**, *25*, 2951.

Table II. Ligand-Field Parameters for Pseudooctahedral Co^{III} Complexes with N_6 and N_3S_3 Donor Ligands (cm^{-1})

ligand	*Dq*	*B*	*β*	*C/B*	ref
NH_3	2287	615	0.56	5.02	53
en	2316	590	0.53	4.91	53
sar	2277	567	0.52	5[a]	4, 18
$(NH_3)_2$sar	2268	590	0.53	5[a]	4, 18
$(NO_2)_2$sar	2274	576	0.52	5[a]	2
9-aneN_3	2345	587	0.53	5[a]	54
(aza)capten	2190	444	0.40	5[a]	43

[a] Assumed for these ligands

are all high-spin, indicating that the ligand can be regarded as generating a weak to medium ligand field. This is confirmed by the electronic spectrum[4,18] of $[Ni((NH_3)_2sar)]^{4+}$, which has three absorption bands at 12 420 cm^{-1} ($^3A_{2g} \rightarrow {}^3T_{2g}$), 19 810 cm^{-1} ($^3A_{2g} \rightarrow {}^3T_{1g}(F)$), and 30 320 cm^{-1} ($^3A_{2g} \rightarrow {}^3T_{1g}(P)$) from which the values $10Dq$ = 12 420 cm^{-1} and the Racah parameter of B = 858 cm^{-1} are estimated. The first band has shoulders at 11 390 and 12 770 cm^{-1} while the second has a shoulder at 20 390 cm^{-1}, indicating that the ideal O_h symmetry has been lowered, probably by trigonal distortion, to D_3. If the shoulder at 11 390 cm^{-1} were assigned to the $^3A_2 \rightarrow {}^1E$ (D_3) transition in which both states have the $t_2^6e^2$ configuration, the interelectronic repulsion parameter,[52] B_{33} = 728 cm^{-1}, would be obtained. These parameters are virtually identical with those reported[41] for the pseudooctahedral Ni^{II} complex of the cyclic tridentate 1,4,7-triazacyclononane, which are about 20% larger than the corresponding parameters for the simple σ-donors NH_3 and ethylenediamine (cf. Table I).

The higher charge of the metal(III) cage complexes leads to strong ligand fields and the low-spin configuration observed for Fe^{III}, Co^{III}, and Ni^{III}. For example, the ligand field parameter $10Dq$ = 22 350 cm^{-1} can be estimated from the energy of the $^4A_{2g} \rightarrow {}^4T_{2g}$ absorption band[15] of the complex $[Cr((NH_3)_2sar)]^{5+}$. Perhaps surprisingly, complexes of $[Mn\ sar]^{3+}$ in which the octahedra are considerably distorted, presumably by Jahn–Teller instability, are found to be high spin, but it is believed that they must lie close to the $3d^4$ spin crossover.

Generally, the $\mu(T)$ behavior observed for these cage complexes is similar to that published for related hexaamine complexes and is consistent with a pseudooctahedral geometry that has undergone further distortion. These distortions are evident in the zero-field splitting of orbital singlet ground states observed in the magnetism at low temperatures.

The diamagnetism of $[Fe((NH_2)_2sar)](CF_3SO_3)_2$ contrasts sharply with the fully developed paramagnetism of $[Fe(sar)](CF_3SO_3)_2$, $[Fe((NH_3)_2sar)]Br_2Cl_2 \cdot 4H_2O$, and $[Fe((Me)sar)](CF_3SO_3)_2$. Since it is unlikely that the ligand-field strength for this complex differs significantly from that of the three high-spin Fe^{II} cages, all four Fe^{II} complexes must lie very close to the spin-crossover region, with lattice and solvation effects being the salient factors in determining their ultimate spin state either in the crystal or in solution. Indeed, recent measurements of magnetism and visible and NMR spectra confirm that all the $Fe^{II}N_6$ cages of this type exhibit a spin equilibrium in solution[4,32] of $^5T_{2g} \rightleftarrows {}^1A_{1g}$ origin in O_h symmetry.

The low-spin configuration observed for $[Co((aza)capten)]^{2+}$ warrants further discussion of the relative strength of the ligand field for the $Co^{II}N_3S_3$ cage since the $Co^{II}N_6$ type cages are high spin. The low-spin ground state appears to be caused mainly by the smaller value of the Racah interelectronic repulsion parameter B as a result of increased covalency when nitrogen is partly replaced by sulfur although a small decrease in $10Dq$ also occurs. These nephelauxetic and ligand-field effects are clearly evident in the ligand-field parameters listed in Table II, which can be derived from the electronic spectra of cobalt(III) complexes;[4,18] the ratios are $[10Dq]_{N_6}/[10Dq]_{N_3S_3}$ = 1.04 and $[B]_{N_6}/[B]_{N_3S_3}$ = 1.30, respectively.

The spectrum of low-spin $[Co((aza)capten)]^{2+}$ has bands at 12 800, 18 200, and 20 000 cm^{-1}, which have tentatively been ascribed to $^2E_g \rightarrow {}^4T_{1g}(F)$, $^2E_g \rightarrow {}^2T_{1g}(G)$ and $^2E_g \rightarrow {}^2T_{2g}(G)$ transitions, respectively.[43] However, this assignment of the low-energy band leads to estimates of $10Dq$ that are unrealistically high. Since the ^2E_g ground state is likely to undergo an appreciable Jahn–Teller splitting, perhaps induced by a tetragonal distortion of the N_3S_3 octahedron, the estimated high-spin–low-spin separation[41] would become $4B + 4C - 10Dq - 2E_{JT}$. If we assume for $[Co((aza)capten)]^{2+}$ that its $10Dq$ and B parameters were reduced compared to those for $[Co((NH_3)_2sar)]^{4+}$ in the same ratios found for the Co^{III} cages, the values $10Dq \sim 11\,000$ and $B \sim 624$ cm^{-1} would be obtained. Wieghardt et al.[41] report values of $4E_{JT}$ that range from 7500 cm^{-1} for $[Co(terpy)_2]^{2+}$ salts to 13 600 cm^{-1} for the Co^{II} complex of the monooxa analogue of 1,4,7-triazacyclononane. If we assume that the electronic band at 12 800 cm^{-1} arises not from a transition between ^2E_g and $^4T_{1g}$ levels but rather from one between $^2A_{1g}$ and $^2B_{1g}$ levels in D_{4h} symmetry, then $4E_{JT}$ = 12 800 cm^{-1}. Then the estimated energy separation between high-spin and low-spin levels is calculated to be negative (−4000 cm^{-1}) as required for the observed low-spin ground state. Thus although $10Dq$ is probably lowered slightly from 11 570 (N_6) to 11 000 (N_3S_3) cm^{-1}, the combination of a significant decrease in B from 800 to 624 cm^{-1} and a large Jahn–Teller splitting of the ^2E_g level is sufficient to stabilize a low-spin ground state, which is found for the cage $[Co((aza)capten)]^{2+}$. Interestingly, in their comparison of high-spin $[Co(9\text{-ane}N_3)_2]^{2+}$ and its low-spin S_6 analogue, $[Co(9\text{-ane}S_3)_2]^{2+}$, Wieghardt et al.[41] concluded that although B is lowered from 780 to 730 cm^{-1} for the S_6 complex, $10Dq$ is actually increased from 12 000 to 13 500 cm^{-1} with the Jahn–Teller splitting $4E_{JT}$ remaining essentially unchanged at about 7000 cm^{-1}.

Acknowledgment. We wish to thank K. Berry, and Drs. B. J. Kennedy and E. N. Bakshi for help with computer fitting methods and helpful discussions, A. C. McGrath, P. Zwack, and C. Delfs and Dr. A. Markiewicz for experimental assistance, and Drs. I. I. Creaser, L. R. Gahan, K. S. Hagen, M. McCarthy, and G. A. Lawrance for providing some samples used in this study. K.S.M. is grateful for financial support from the Australian Research Grants Scheme, and we are grateful for critical comments from Dr. R. Bramley and the reviewers.

(52) Jørgensen, C. K. *Modern Aspects of Ligand Field Theory*; North Holland: Amsterdam, 1971.
(53) Lever, A. P. B. *Inorganic Electronic Spectroscopy*; Elsevier: Amsterdam, 1984.
(54) Nonoyama, M.; Sakai, K. *Inorg. Chim. Acta* **1983**, *72*, 57.